Journal of Molecular Structure 1010 (2012) 1–7

Contents lists available at SciVerse ScienceDirect

Journal of Molecular Structure

journal homepage: www.elsevier.com/locate/molstruc

Synthesis, crystal structure, antibacterial activities, and electrochemical studies of new N,N′-polymethylene bis-sulfonamides

Neslihan Özbek [a], Saliha Alyar [b], Serhat Mamaş [c], Ertan Şahin [d], Nurcan Karacan [c,*]

[a] Department of Primary Education, Faculty of Education, Ahi Evran University, TR-40100 Kırşehir, Turkey
[b] Department of Chemistry, Science and Art Faculty, Karatekin University, TR-18100 Çankırı, Turkey
[c] Department of Chemistry, Faculty of Science, Gazi University, TR-06500 Ankara, Turkey
[d] Department of Chemistry, Faculty of Science and Art, Atatürk University, TR-25240 Erzurum, Turkey

ARTICLE INFO

Article history:
Received 2 August 2011
Received in revised form 19 October 2011
Accepted 20 October 2011
Available online 11 November 2011

Keywords:
Bis-sulfonamides
Antimicrobial activity
Cyclic voltammetry
X-ray structure

ABSTRACT

Four disulfonamide derivatives $(C_2H_5{\cdot}SO_2{\cdot}NH)_2(CH_2)_n$ (n = 2, 3, 4, 5) were synthesized and characterized by FTIR, ^{1}H NMR, ^{13}C NMR, HETCOR, LCMS and elemental analysis. *Ethanesulfonamide-N,N′-pentamethylene bis* was also characterized by X-ray single crystal diffraction measurement. The electrochemical characteristics of the disulfonamide derivatives were performed by cyclic voltammetry and chronoamperometry. ^{1}H and ^{13}C NMR chemical shifts of the compounds were calculated by using DFT/B3LYP methods with a 6-311++G (d,p) basis set. Antibacterial activity and the structural relationship of the compounds showed that activity decreases proportionately to the increasing length of the carbon chain between NH groups, log*P* values, hydration energy and molecular volumes. Anodic peak potentials and HOMO values do not correlate with the activity, but reduction potential and LUMO decrease weakly with increasing activity.

1. Introduction

Sulfonamides were the first effective chemotherapeutic agents employed systematically for the prevention and cure of bacterial infections in humans and other animal systems [1–3]. Despite the loss of value in the development of antimicrobial therapy over time, the synergetic action of sulfonamides with trimethoprim has brought about widespread usage over the last decade [4]. The discovery of novel antimicrobial agents with better pharmacological profiles is still highly desirable, due to the evolution of drug resistance [5,6] and the threat of bioterrorism [7].

Knowledge on the antimicrobial activity of bis-sulfonamides appears to be limited in the literature [8,9]. Wilkinson et al. showed that a bis-arylsulfonamide exhibits moderate growth inhibition against *Mycobacterium smegmatis* [10]. Asundaria et al. reported that 4-sulfonamides substituted novel sydnones show excellent antibacterial activity against Gram pos. *Staphylococcus pneumoniae* and *Staphylococcus aureus*, and Gram neg. bacteria *Escherichia coli* and *Pseudomonas aeruginosa* [11].

In our previous studies, aliphatic/aromatic bis sulfonamides were synthesized and tested for antimicrobial activity [12–16]. Continuing our studies, in this paper a series of new N,N′-polymethylene bis-sulfonamide derivatives (indicated as n = 2: ESEN, n = 3: ESPR, n = 4: ESBUT, and n = 5: ESPEN) (Fig. 1) were synthesized and characterized by elemental analysis, and FT-IR, ^{1}H NMR, ^{13}C NMR, 2D-HETCOR and LC–MS methods. Electrochemical properties of the compounds were studied by cyclic voltammetry and chronoamperometry. Their antibacterial activities were evaluated against Gram-positive bacteria (*S. aureus* ATCC 25923, *Bacillus cereus* RSKK 863, *Bacillus subtilis* ATCC 6633, *Listeria monocytogenes* ATCC Li6 (izolate) and Gram-negative bacteria (*E. coli* ATCC 11230, *Salmonella enteritidis* ATCC 13076, *P. aeruginosa* ATCC 27853 and *Yersinia enterocolitica* O:3) by both disc diffusion and micro dilution methods. The crystal structure of **ESPEN** was investigated by X-ray analysis. Theoretical chemical shifts of the compounds were calculated by using DFT/B3LYP methods with a 6-311++G (d,p) basis set to support the examination.

2. Experimental

2.1. Chemistry

The elemental analyses (C, H, N and S) were performed on a LECO–CHSNO – 9320 type elemental analyzer. The IR spectra (4000–400 cm^{-1}) were recorded on a Mattson-1000 FT-IR spectrophotometer with samples prepared as KBr pellets. NMR spectra were recorded on a Bruker-Spectrospin Avance DPX – 400 Ultra – Shield (400 MHz) by using DMSO as a solvent and TMS as an internal standard. LC/MS-APCl was recorded on the AGILENT 1100. The melting point was recorded on Opti Melt apparatus. TLC was conducted on 0.25 mm silica gel plates (60F254, Merck). Visualization was made by using ultraviolet light. All extracted solvents (all from

* Corresponding author. Tel.: +90 312 2021117; fax: +90 312 2122279.
E-mail address: nozbek@gazi.edu.tr (N. Karacan).

0022-2860/$ - see front matter © 2011 Elsevier B.V. All rights reserved.
doi:10.1016/j.molstruc.2011.10.040

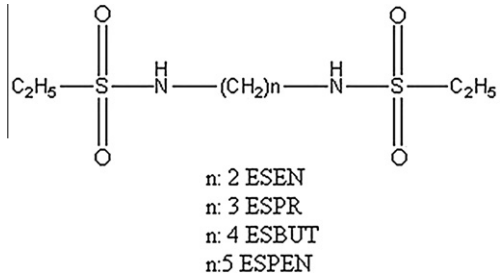

Fig. 1. Structure of the compounds.

Merck) were dried over anhydrous Na_2SO_4 and evaporated by using a BUCHI rotary evaporator. Reagents were obtained commercially from Aldrich (ACS grade) and used as received.

2.2. General procedure for the synthesis

Nucleophilic substitution reactions of aliphatic diamines with alkyl sulfonyl chlorides were carried out as follows: Aliphatic diamines in THF were added slowly to sulfonyl chlorides in THF (tetrahydrofurane) at −5 to 0 °C. The reaction mixture was allowed to warm to room temperature and was stirred for 24 h. Completion of the reaction was monitored by TLC, after which the solvent was evaporated in vacuo. The solid residue was purified by column chromatography.

2.2.1. Synthesis of ethanesulfonamide-N,N′-dimethylenebis (ESEN)

The white crystalline solid synthesized from 1,2-diamino ethane (3.0 mL, 0.032 mol) and ethanesulfonyl chloride (4.2 mL, 0.063 mol) was recrystallized from a tetrahydrofurane (THF)/*n*-hexane (3/1) mixture. The product was dried in vacuum and stored in THF vapor. Yield 75%; mp 153–155 °C; Analytical and physical data: $C_6H_{16}N_2O_4S_2$; C, 29.58; H, 6.54; N, 11.53; S, 26.17. Calculated C, 29.51; H, 6.55; N, 11.47; S, 26.23. MS (70 eV, APCl): 245.1 $(M+1)^{+\cdot}$, 245.9 $(M+2)^{+\cdot}$, 247.0 $(M+3)^+$, 106.15 $[CH_3CH_2SO_2N\text{-}1]^+$, 122.0 $[CH_3CH_2SO_2NHCH_2]^+$, 136.10 $[M—NHSO_2CH_2CH_3]^+$. IR (KBr) cm^{-1}: 3268 υ(NH), 1470 δ(NH), 2975 $\upsilon(CH_3)$, 1318 $\upsilon_{as}(SO_2)$, 1136 $\upsilon_s(SO_2)$.

2.2.2. Synthesis of ethanesulfonamide-N,N′-threemethylenebis (ESPR)

The white crystalline solid synthesized from 1,3-diamino propane (3.0 mL, 0.032 mol) and ethanesulfonyl chloride (5.3 mL, 0.063 mol) was recrystallized from a THF/*n*-hexane (3/1) mixture. The product was dried in vacuum and stored in THF vapor. Yield 70%; mp 158–160 °C; Analytical and physical data: $C_7H_{18}N_2O_4S_2$; C, 32.70; H, 7.11; N, 10.94; S, 24.75. Calculated C, 32.56; H, 6.98; N, 10.85; S, 24.80. MS (70 eV, APCl): 259.05 $[M+1]^+$, 260.05 $[M+2]^+$, 261.0 $[M+3]^+$, 122.0 $[CH_3CH_2SO_2NHCH_2]^+$, 150.10 $[M—NHSO_2CH_2CH_3]^+$. IR (KBr) cm^{-1}: 3242 υ(NH), 1460 δ(NH), 2974 $\upsilon(CH_3)$, 1314 $\upsilon_{as}(SO_2)$, 1142 $\upsilon_s(SO_2)$.

2.2.3. Synthesis of ethanesulfonamide-N,N′-tetramethylenebis (ESBUT)

The white crystalline solid synthesized from 1,4-diaminobutane (3.0 mL, 0.032 mol) and ethanesulfonyl chloride (6.4 mL, 0.064 mol) was recrystallized from an ethanol/*n*-hexane (4/1) mixture. The product was dried in vacuum and stored in ethanol vapor. Yield 75%; mp 171–173 °C; Analytical and physical data: $C_8H_{20}N_2O_4S_2$; C, 35.38; H, 7.22; N, 10.32; S, 23.42. Calculated C, 35.29; H, 7.35; N, 10.29; S, 23.52. MS (70 eV, APCl): 273.10 $[M+1]^+$, 274.1 $[M+2]^+$, 275.1 $[M+3]^+$, 122.0 $[CH_3CH_2SO_2NHCH_2]^+$. IR (KBr) cm^{-1}: 3241 υ(NH), 1442 δ(NH), 2977 $\upsilon(CH_3)$, 1309 $\upsilon_{as}(SO_2)$, 1142 $\upsilon_s(SO_2)$.

2.2.4. Synthesis of ethanesulfonamide-N,N′-pentamethylenebis (ESPEN)

The white crystalline solid synthesized from 1,5-diaminopentane (3.0 mL, 0.032 mol) and ethanesulfonyl chloride (4.0 mL, 0.064 mol) was recrystallized from an ethanol/*n*-hexane (4/1) mixture. The product was dried in vacuum and stored in ethanol vapor. Yield 82%; mp 178–180 °C; Analytical and physical data: $C_9H_{22}N_2O_4S_2$; C, 37.89; H, 7.56; N, 9.77; S, 22.24. Calculated C, 37.76; H, 7.69; N, 9.79; S, 22.37. MS (70 eV, APCl): 287.10 $[M+1]^+$, 288.1 $[M+2]^+$, 289.1 $[M+3]^+$,193.10 $[M—SO_2CH_2CH_3]^+$. IR (KBr) cm^{-1}: 3273 υ(NH), 1460 δ(NH), 2976 $\upsilon(CH_3)$, 1316 $\upsilon_{as}(SO_2)$, 1148 $\upsilon_s(SO_2)$.

2.3. Crystal structure determination

For the crystal structure determination, the single-crystal of the compound ESPEN was used for data collection on a four-circle Rigaku R-AXIS RAPID-S diffractometer (equipped with a two-dimensional area IP detector). The graphite-monochromatized Mo Kα radiation (λ = 0.71073 Å) and oscillation scans technique with $\Delta\omega = 5°$ for one image were used for data collection. The lattice parameters were determined by the least-squares methods on the basis of all reflections with $F^2 > 2\sigma(F^2)$. Integration of the intensities, correction for Lorentz and polarization effects and cell refinement was performed using Crystal Clear (Rigaku/MSC Inc., 2005) software [17]. The structure was solved by direct methods using SHELXS-97 and refined by a full-matrix least-squares procedure using the program SHELXL-97 [18]. All H atoms attached to C atoms were fixed geometrically and treated as riding with C—H = 0.97 Å (methylene) or 0.96 Å (methyl) with *U*iso(H) = 1.2*U*eq(methylene) and 1.5*U*eq(-methyl) of the parent atom. The N protons were located in Fourier difference maps and constrained as riding atoms with N(1)—H(1N) and N(2)—H(2N) set to 0.83 and 0.967 Å respectively. The final difference Fourier maps showed no peaks of chemical significance. Crystal data and structure refinement parameters of compound ESPEN were given in Table 1.

2.4. Antimicrobial screening

S. aureus ATCC 25923, *B. cereus* RSKK 863, *B. subtilis* ATCC 6633, Listeria monocytogenes ATCC Li6 (isolate) and Gram-negative

Table 1
Crystal data and structure refinement for ESPEN.

Empirical formula	$C_9H_{22}N_2O_4S_2$
Formula weight	286.4
Temperature	293(2) K
Wavelength	0.71073 Å
Crystal system	Monoclinic
Space group	$P2_1/a$
Unit cell dimensions	a = 11.4820(6) Å, α = 90° b = 9.0430(16) Å, β = 92.79(3)° c = 13.7820(16) Å, γ = 90°
Volume	1429.32(12) $Å^3$
Z	4
Density (calculated)	1.33 Mg/m^3
Absorption coefficient	0.378 mm^{-1}
$F(000)$	616
Crystal	Needle; yellow
Crystal size	0.20 × 0.02 × 0.02 mm^3
θ-Range for data collection	2.70–30.70°
Index ranges	$-15 \leqslant h \leqslant 16$, $-12 \leqslant k \leqslant 12$, $-19 \leqslant l \leqslant 19$
Reflections collected	40150
Independent reflections	4286 [R_{int} = 0.105]
Completeness to θ = 30.7°	99.7%
Max. and min. transmission	0.927 and 0.873
Refinement method	Full-matrix least-squares on F^2
Data/restraints/parameters	4286/0/159
Goodness-of-fit on F^2	1.249
Final R indices [$F^2 > 2\sigma(F^2)$]	R_1 = 0.087, wR_2 = 0.228
R indices (all data)	R_1 = 0.123, wR_2 = 0.254
Extinction coefficient	0.009
Largest diff. peak and hole	0.704 and −0.401 e $Å^{-3}$

bacteria (*E. coli* ATCC 11230, *S. enteritidis* ATCC 13076, *P. aeruginosa* ATCC 27853 and *Y. enterocolitica* O:3) were used as test bacteria. Nutrient Broth (NB) was used for culturing of test bacteria. All strains were stored at −20 °C in the appropriate medium containing 10% glycerol and regenerated twice before use in the manipulations.

2.4.1. Determination of Minimal Inhibitory Concentration (MIC)

A micro dilution broth susceptibility assay was used [19]. Stock solutions of the test compounds were prepared in 10% dimethylsulfoxide (DMSO) and then serial dilutions of the test compounds were made in a concentration range from 200 to 1400 μg/mL. The 96-well plates were prepared by dispensing into each well 95 μL of nutrient broth and 5 μL of the inoculum. One-hundred microliters from each of the test compounds initially prepared at a concentration of 1400 μg/mL was added into the first wells. The last well containing 195 μL of nutrient broth without compound and 5 μL of the inoculum on each strip was used as negative control. The final volume in each well was 200 μL. The contents of the wells were mixed and the micro plates were incubated at 37 °C for 24 h. All of the compounds tested in this study were screened twice against each microorganism. The MIC was defined as the lowest concentration of the compounds to inhibit the growth of microorganisms.

2.4.2. Disc diffusion method

The synthesized and lyophilized compounds were dissolved in dimethylsulfoxide (10% DMSO) to a final concentration of 6 mg/mL and sterilized by filtration by 0.45 mm millipore filters. The culture suspensions were adjusted by comparing against 0.5 McFarland. The discs (6 mm in diameter) were impregnated with 10 μL of each compound (60 μg/disc) at the concentration of 6 mg/mL and placed on the inoculated agar. DMSO impregnated discs were used as negative controls. Ciprofloxacin (5 μg/disc), Ampicillin (10 μg/disc) and Penicillin (10 units) were used as standard drugs (positive control). The susceptibility of bacteria to the test compounds was determined by the formation of an inhibitory zone after 24 h of incubation at 37 °C. Antimicrobial activity in a disc diffusion assay was evaluated by measuring the zone of inhibition against the test organisms. Each assay in this experiment was repeated twice [20].

2.5. Electrochemical studies

Voltammetric measurements were performed using an Ivium Stat potentiostat. A glassy carbon working electrode (BAS; ∅: 3 mm, diameter), a commercial Ag/Ag^+ (BAS Co., Ltd.) reference electrode, a platinum wire counter electrode, and a standard one-compartment three-electrode cell of 10 mL capacity were used in all experiments. Before each measurement, the glassy carbon electrode was polished manually with an aqueous slurry of alumina powder (∅: 0.01 μm) on a damp smooth polishing cloth (BAS velvet polishing pad). All measurements were realized at room temperature. 0.1 M tetrabutylammonium tetraflouroborate (TBATFB) was used as supporting electrolyte. 10^{-3} M of the compounds was dissolved in the DMSO. The ultra micro electrode (UME) studies were carried out using 10 μm diameter Pt ultra micro disc electrodes. The UME responses and chronoamperometric Cottrell slopes of the 1 mM ligand on the Pt disc electrodes were used to determine the diffusion coefficients and number of electrons transferred.

3. Results and discussion

3.1. Crystal structure

An X-ray diffraction analysis of *ethanesulfonamide-N,N′-pentamethylenebis* (ESPEN) was undertaken. The compound crystallized in the monoclinic space group $P2_1/a$ with four molecules in the unit cell (Fig. 2). In the structure, the main chain is represented by a zig-zag line near to the plane maximum deviation from N1/C3—C7/N2 mean plane is −0.142 Å for atom N1). Terminal ethanesulfonamide fragments were forced back to the opposite sides. In the sulfonyl unit, the S═O bond lengths are a bit longer than in our previous structure [21] while the S—N and S—C bond lengths have shorter values.

The crystal structure consists of layers where the sulfonamide atoms are involved in hydrogen bond network. Namely, the sulfonamide group is involved in two hydrogen bonds (between sulfonamide O atoms and nitrogen atoms) with two different symmetry-related molecules, building a two dimensional network parallel to the crystal plane [101]. (Table 2, Fig. 3). Similar *N—H···O* hydrogen bonds are observed in the other structures containing sulfonamide groups [22,23].

3.2. NMR spectra

In this study, the magnetic isotropic shielding tensors (δ_C) of the compounds were calculated for the most stable conformers using GIAO /B3LYP/6-311++G (d,p) and IEF-PCM methods in dimethylsulfoxide (DMSO) solutions with GAUSSIAN03 software [24] to assist in the assignment of chemical shifts of carbon atoms. All the experimental and calculated shielding values of the compounds are given in Table 3. There is a relationship between order of chemical shift of C and H atoms, except CH_2 groups bonding to S and N atoms. The 2D HETCOR was used to confirm the chemical shift in the NMR spectra. The HETCOR spectrum of ESPEN in DMSO-d_6 is given in Fig. 4. The chemical shift at 45.67 ppm and 42.66 ppm in the ^{13}C NMR spectrum belongs to the S—**C**H_2 and N—**C**H_2 groups, respectively. However, the 2D HETCOR spectrum showed that the signals at 2.90 and 2.98 ppm correspond to the S—**C**H_2 and N—**C**H_2 groups, respectively. We calculated ^1H chemical shift values (with respect to TMS) of S—C**H₂** and N—C**H₂** at 3.11 and 3.09 ppm. According to these results, the calculated chemical shifts are in compliance with the experimental findings. The correlation graphic based on the calculated values and experimental data of **(ESPEN)** data is also been given in Figs. 5 and 6. The correlation values for proton and carbon chemical shifts were measured as 0.997 and 0.988 for B3LYP with the 6-311++G (d,p) basis set.

3.3. Antimicrobial activity

The MIC values and inhibition zones (mm) of the compounds are listed in Tables 4 and 5. Commonly used antibiotics Ciprofloxacin, Ampicillin and Penicillin were tested as positive controls. ESEN showed the best activity with the lowest MIC (465 μg/mL) against *E. coli* bacteria. The antimicrobial activity results indicate that (a) bis-sulfonamides showed relatively better activity against Gram-negative bacteria than Gram-positive bacteria, and (b) antibacterial

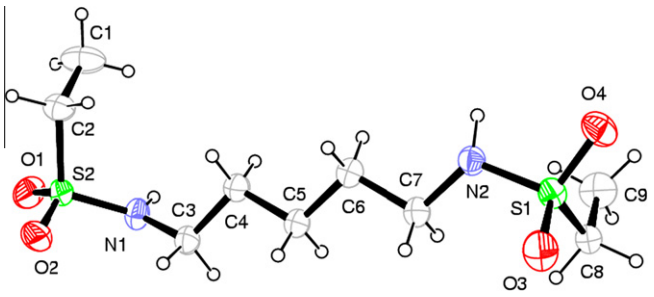

Fig. 2. The molecular structure of ESPEN with the atom-numbering scheme; displacement ellipsoids are drawn at the 50% probability level.

Table 2
Selected bond lengths (Å) and angles (°), and hydrogen bonds for ESPEN.

Bond lengths			
S(1)—O(4)	1.431(4)	S(1)—N(2)	1.618(4)
S(1)—O(3)	1.438(4)	S(1)—C(8)	1.762(5)
S(2)—O(2)	1.441(4)	S(2)—N(1)	1.595(4)
S(2)—O(1)	1.438(5)	S(2)—C(2)	1.764(5)
N(1)—C(3)	1.459(5)	N(2)—C(7)	1.473(5)
Bond angles			
O(4)—S(1)—N(2)	106.5(3)	O(4)—S(1)—O(3)	118.5(3)
O(4)—S(1)—C(8)	109.2(3)	N(2)—S(1)—O(3)	108.0(3)
N(2)—S(1)—C(8)	107.8(3)	O(3)—S(1)—C(8)	106.4(3)
O(2)—S(2)—N(1)	107.3(3)	O(2)—S(2)—O(1)	119.9(3)
N(1)—S(2)—C(2)	110.5(3)	O(2)—S(2)—C(2)	106.4(4)
Hydrogen bonds			
D—H···A	*d*(H···A)	*d*(D···A)	<(DHA)
N(1)—H(1N)···O(2)[a]	0.83	2.926(6)	169
N(2)—H(2N)···O(3)[b]	0.97	2.952(6)	171

Symmetry transformations used to generate equivalent atoms:
[a] $-1/2-x, 1/2+y, -z$.
[b] $1/2-x, 1/2+y, 1-z$.

activity decreased proportionately to the increasing length of the carbon chain between NH groups [14]. In order to find correlations between some physicochemical parameters and antimicrobial activity, some selected parameters (log*P*, molecular volume, hydration energy, heat of formation energy, HOMO, LUMO, and charge of **N**H) were calculated using Hyperchem software [25] and are tabulated in Table 6. Both the octanol–water partition coefficient (log*P*) and the hydration energy have been considered as descriptors of the hydrophobic effect. As shown in Table 6, log*P* values, hydration energy, and the molecular volumes increase with a decrease in activity of the compounds. The most active compound (ESEN) had the lowest value of molecular volume. So, using substituents that increase the hydrophobicity of the compound should be avoided. Heat of formation energy is a thermodynamic parameter and accounts for the chemical stability of the molecule. In our series, activity increases with increasing heat of formation energy, in other words activity increases with decreasing stability. In addition, HOMO values do not correlate with the activity. However, LUMO values decrease weakly with increasing activity. This result shows that the bis sulfonamides act as Lewis acids while interacting with enzymes in the bacteria.

3.4. Electrochemical studies

Cyclic voltammograms of the sulfonamide derivatives are depicted in Fig. 7, and the plots of the logarithm of the cathodic current responses (i_{pc}) vs. the logarithm of the scan rate (v), with their regression line equations for each compound, are given in Fig. 8. As

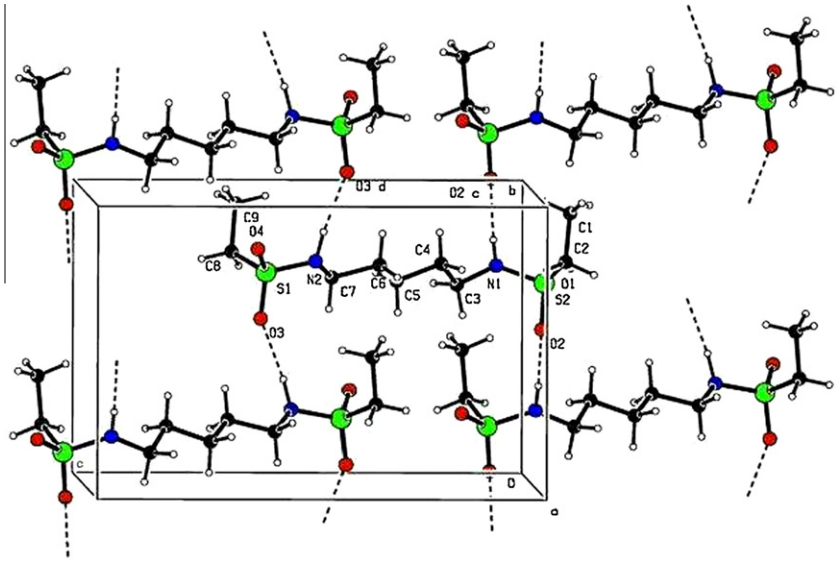

Fig. 3. Crystal packing and the H-bonding geometry parallel to the crystal plane [1 0 1]. H-bonds are indicated by dot lines.

Table 3
^{1}H and ^{13}C chemical shifts (ppm) and calculated GIAO/B3LYP/6-311G (d,p) magnetic isotropic ^{13}C shielding tensors in DMSO (*: Average values).

Assignment	ESEN		ESPR		ESBUT		ESPEN	
	$\delta_{(exp.)}$	$\delta_{(calc.)}$	$\delta_{(exp.)}$	$\delta_{(calc.)}$	$\delta_{(exp.)}$	$\delta_{(calc.)}$	$\delta_{(exp.)}$	$\delta_{(calc.)}$
C atoms								
$\langle CH_3\rangle$	8.24	9.50	8.25	9.88	8.30	9.89	8.55	9.47
$CH_3\langle CH_2\rangle$	47.12	51.04	46.61	50.01	46.79	49.58	45.67	48.97
$NH\langle CH_2\rangle$	43.68	46.80	39.87	43.51	42.67	44.69	42.66	45.64
$NHCH_2\langle CH_2\rangle$	–	–	30.97	39.14	27.27	30.67	29.46	35.42
$NHCH_2CH_2\langle CH_2\rangle$	–	–	–	–	–	–	23.67	27.96
H atoms								
$\langle CH_3\rangle$	1.35(t, 3H)	1.23*	1.34(t, 3H)	1.22*	1.37(t, 3H)	1.21*	1.19(t, 3H)	1.19*
$CH_3\langle CH_2\rangle$	3.01(q, 2H)	2.96*	3.04(q, 2H)	2.98*	3.07(q, 2H)	2.99*	2.98(q, 2H)	3.11*
$NH\langle CH_2\rangle$	3.23(q, 2H)	3.16*	3.22(q, 2H)	3.24*	3.16(q, 2H)	3.19*	2.90(q, 2H)	3.09*
$NHCH_2\langle CH_2\rangle$	–	–	1.78(m, 2H)	1.68*	1.68(m, 2H)	1.58*	1.45(m, 2H)	1.56*
$NHCH_2CH_2\langle CH_2\rangle$	–	–	–	–	–	–	1.32(m, 2H	1.47
NH	6.77	5.51*	6.75	5.72*	6.71	5.79*	6.80	5.68*

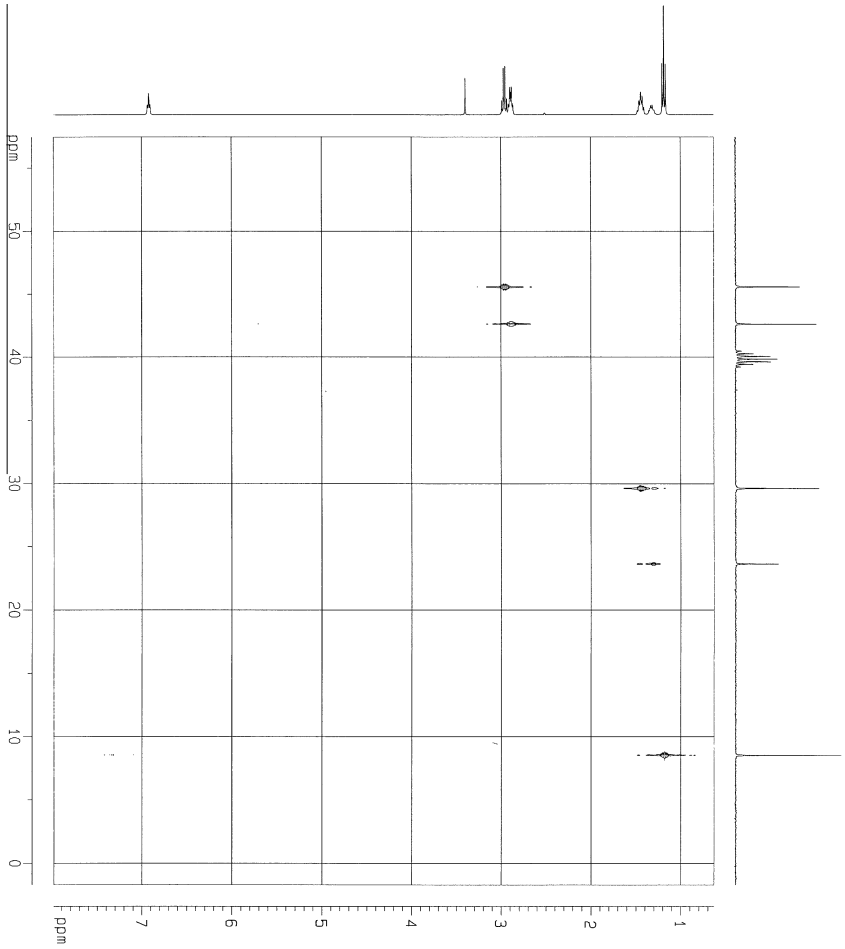

Fig. 4. HETCOR spectrum of ESPEN.

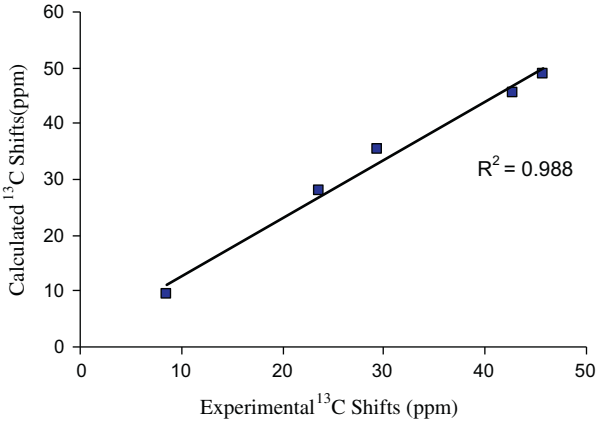

Fig. 5. Plot of the calculated vs. the experimental ^{13}C NMR chemical shifts of (ESPEN).

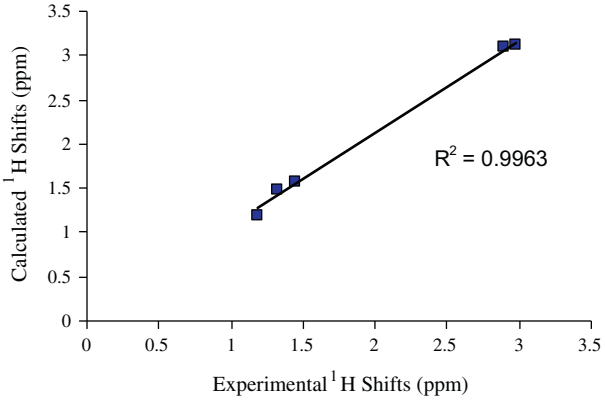

Fig. 6. Plot of the calculated vs. the experimental ^{1}H NMR chemical shifts of (ESPEN).

can be seen from the equation of the regression lines, the slopes of $\log i_{pc}$ vs. $\log v$ are equal to approximately 0.5 for all derivatives, indicating that the reduction of the compounds are diffusion controlled at the glassy carbon surface in DMSO.

The number of electrons transferred (n) in the electrochemical reduction are obtained using the equation $n = \frac{s^2\pi 4r}{i_{ss}FA^2C}$ which is valid for ultra microelectrodes (UME) in chronoamperometric experiments [26].

I_{ss} values of ESEN, ESPR, ESBUT and ESPEN were obtained from Fig 9. and presented in Table 7. The Cottrell slopes (S) in Table 7

Table 4
Antimicrobial activity of compounds with micro dilution method (μg/mL).

Test bacteria	ESEN	ESPR	ESBUT	ESPEN
Escherichia coli ATCC 11230	465	515	556	612
Salmonella enteritidis ATCC 13076	560	630	640	770
Listeria monocytogenes Li6 (isolate)	560	630	770	840
Bacillus cereus RSKK863	534	589	626	753
Staphylococcus aureus ATCC 25923	534	589	626	703

Table 5
Inhibition zones of compounds and reference antibiotics discs against tested microorganisms by disc diffusion method (disc potency 60 μg).

Compounds	Diameter of inhibition zone (mm)				
	EC	*SE*	*LM*	*BC*	*SA*
ESEN	18	17	12	11	10
ESPR	17	16	10	10	10
ESBUT	17	16	9	9	9
ESPEN	15	12	9	8	8
Ciprofloxacin	36	30	12	26	29
Penicillin	17	18	11	8	14
Ampicillin	11	12	13	13	15

Table 6
Some calculated physicochemical properties of the compounds.

	ESEN	ESPR	ESBUT	ESPEN
Log *P*	−0.56	−0.51	−0.06	0.34
Molecular volume (A^3)	672.11	757.62	821.43	860.24
Hydration energy (kcal/mol)	−9.61	−9.25	−8.98	−8.54
Heat of formation (kcal/mol)	−157.41	−161.41	−167.12	−172.94
LUMO (au)	−0.67	−0.53	−0.47	−0.43
HOMO (au)	−10.31	−10.31	−10.32	−10.32
Charge on **N**H	−0.504	−0.503	−0.503	−0.502

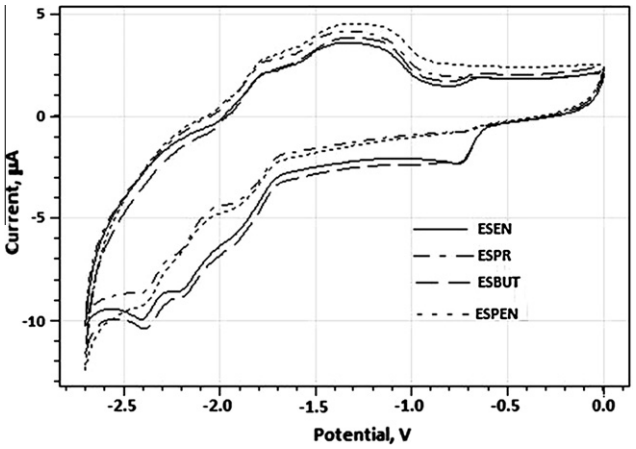

Fig. 7. The cyclic voltammograms for 1 mM of ESEN, ESPR, ESBUT and ESPEN in DMSO at scan rate of 0.1 V/s.

were obtained from plots given in Fig. 10 which were acquired from the chronoamperometric experiments. The values obtained from Fig. 9 and Fig. 10 are tabulated in Table 7.

The number of electrons transferred for the compounds was found to be approximately 2 for all derivatives. This value is comparable to the values reported in literature [26,27]. It is considered as the number of electrons transferred in the first step of reduction of sulfonamide species to give their corresponding stable anions. In the second reduction step at higher potentials, dianions are produced and rapidly decomposed to sulfinates and amide anions.

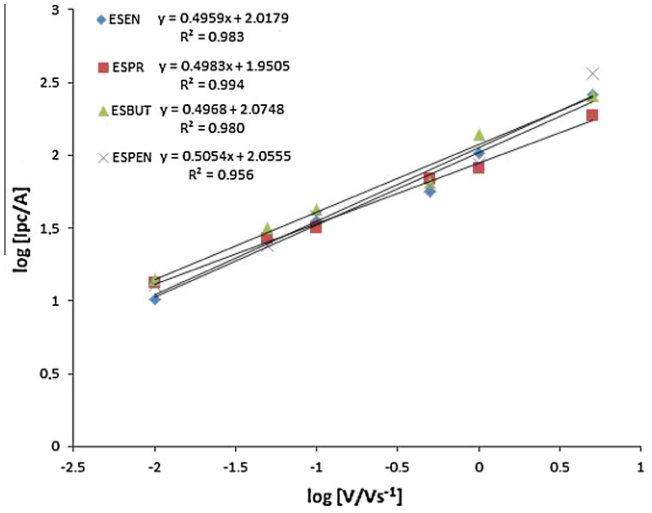

Fig. 8. Plots of $\log i_{pc}$ vs. $\log v$ for compounds 1 mM of ESEN, ESPR, ESBUT and ESPEN reduced in DMSO at GC.

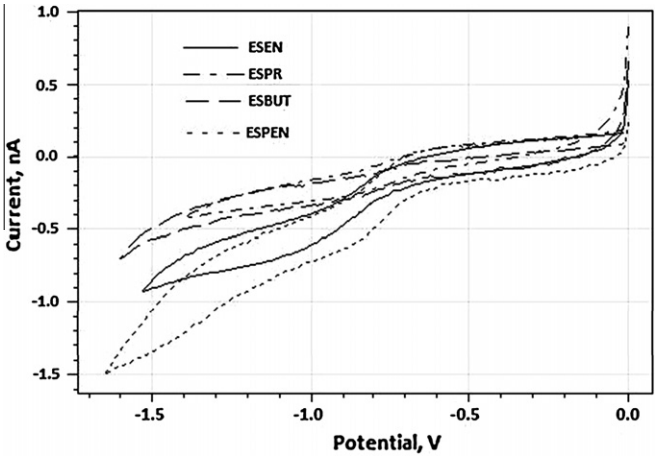

Fig. 9. Steady state voltammograms of 1 mM of ESEN, ESPR, ESBUT and ESPEN at Pt Ultra micro disc electrode (UME) at scan rate of 0.025 V/s.

It is noteworthy to point out here that the diffusion coefficients of the sulfonamide derivatives obtained from the Cottrell slopes are in accordance with their molecular weights. These are expected results because the increase in the carbon chain increases the molecular weight, which is inversely related to the diffusion coefficient.

Anodic peak potentials of the compounds are approximately constant (Table 7). We were not surprised to find this result, because the calculated charge on N atoms and HOMO values of the compounds was not significantly changed, as shown in Table 6. On the other hand, the reduction potential of the compounds decreased in opposite ratio to the molecular weight. We also noticed that the reduction potential decreased in parallel with the decrease in LUMO values.

Table 7
Voltammetric parameters obtained for the compounds.

Compound (mass of mole g/mol)	E_{pc} (V)	E_{pa} (V)	Cottrell slope (S)	Limiting current of UME (*i*, A)	Diffusion coefficient ($D_0 \times 10^{-4}$ cm^2/s)
ESEN (245.28)	−2.34	−0.45	1.55×10^{-5}	1.07×10^{-10}	2.89
ESPR (259.30)	−2.27	−0.44	2.72×10^{-5}	3.37×10^{-10}	2.23
ESBUT (273.32)	−2.25	−0.43	3.69×10^{-5}	4.22×10^{-10}	1.76
ESPEN (287.33)	−2.24	−0.42	4.21×10^{-5}	6.14×10^{-10}	1.74

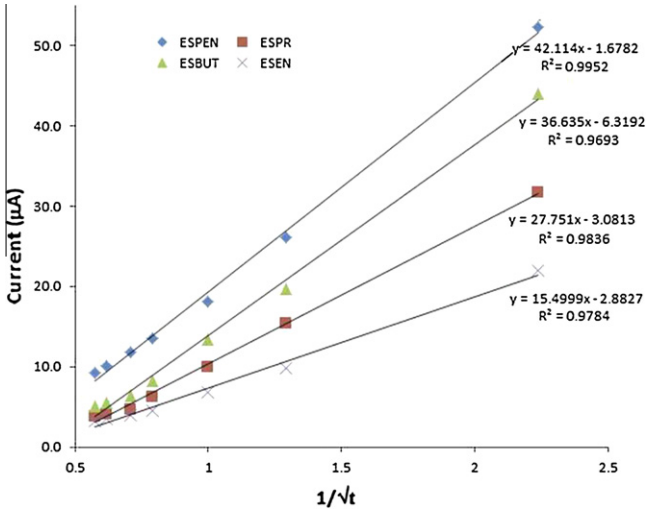

Fig. 10. Chronoamperometric responses of 1 mM of ESEN, ESPR, ESBUT and ESPEN in DMSO at GC.

The Cottrell equation establishes that the slope of I versus sqrt(t) is directly proportional to the electroactive surface, and defined as the ratio between the electrochemical surface and the geometrical surface. These results are also compatible with the expectations that the electroactive surface decreases with increasing antimicrobial activity in parallel to molecular volume.

As seen from Tables 5 and 7, ESEN, ESPR, ESBUT, and ESPEN had both antimicrobial activity and diffusion coefficient (D^o) in decreasing order. Therefore, it may be said that material that can be most rapidly diffused from bulky solution to electrode surface demonstrates the best antimicrobial activity.

4. Conclusion

The antibacterial activity of a series of new bis sulfonamides was screened against Gram-negative and Gram-positive bacteria. As a result, ESEN showed the best activity, with the lowest MIC (465 μg/mL), against *E. coli* bacteria. The structure–activity relationship was investigated by using selected parameters. It was shown that the activity of the compounds decreases by increasing the CH_2 group into the carbon chain of bis sulfonamides, log$P$ values, hydration energy and molecular volumes. Anodic peak potentials and HOMO values do not correlate with the activity, but LUMO decrease weakly with increasing activity. Reducing the potential of the compounds shifts the positive direction in parallel to their increasing diffusivity and increasing antibacterial activity.

5. Supplementary data

Crystallographic data (excluding structure factors) for the structures reported in this article have been deposited with the Cambridge Crystallographic Data Centre as supplementary publication number CCDC 743068. Copies of the data can be obtained free of charge on application to CCDC, 12 Union Road, Cambridge CB2 1EZ, UK (fax: +44 1223 336 033; e-mail: deposit@ccdc.cam.ac.uk).

Acknowledgement

This research was supported by TUBITAK Research Fund under Project No.: 104T390, Gazi University BAP (No. 05/2006-33).

References

[1] M.G. Papich, J.E. Riviere, Veterinary pharmacology and therapeutic, nineth ed., 2009, pp. 835–846.
[2] N.P. Shukla, Biosci. Biotechnol. Res. Asia 1 (2003) 57.
[3] K. Isık, F.O. Koçak, Microbiol. Res. 164 (2009) 49.
[4] J.F. Prescott, Antimicrobial therapy in veterinary medicine, fourth ed., 2006, p. 249.
[5] A. Cerny, W. Pichler, Pharmacoepidem. Dr. S. 7 (1998) 23.
[6] A.E. Cribb, B.L. Lee, L.A. Trepanier, S.P. Spielberg, Adv. Drug React. Toxicol. Rev. 15 (1996) 9.
[7] K. Babaoglu, J. Qi, R.E. Lee, S.W. White, Structures 12 (2004) 1705.
[8] H.T. Zaky, M.I. Mohamed, A.M. Nail, N.G. Kandil, Egyptian J. Chem. 47 (2004) 321.
[9] C. Le Sann, M.A. Gower, A.D. Abell, Mini-Rev. Med. Chem. 4 (2004) 747.
[10] B.L. Wilkinson, L.F. Bornaghi, A.D. Wright, T.A. Houston, S.A. Poulsen, Bioorg. Med. Chem. Lett. 7 (2007) 1355.
[11] S.T. Asundaria, K.C. Patel, Indian J. Chem. B 7 (2010) 960.
[12] S. Alyar, N. Ozbek, K. Kuzukiran, et al., Med. Chem. Res. 20 (2011) 175.
[13] S. Alyar, N. Karacan, J. Enzym. Inhib. Med. Chem. 24 (2009) 986.
[14] N. Ozbek, H. Katırcıoglu, N. Karacan, T. Baykal, Bioorg. Med. Chem. 15 (2007) 5105.
[15] S. Alyar, N. Ozbek, N. Karacan, Drug Future 32 (2007) 126.
[16] N. Ozbek, S. Alyar, N. Karacan, Drug Future 32 (2007) 127.
[17] Rigaku/MSC, Inc., 9009 new Trails Drive, The Woodlands, TX 77381.
[18] G.M. Sheldrick, SHELXS97 and SHELXL97, University of Göttingen, Germany, 1997.
[19] E.W. Koneman, S.D. Allen, W.M. Janda, P.C. Scherckenberger, W.C. Winn, Color atlas and textbook of diagnostic microbiology, Philadelphia Lippincott-Raven, 1997.
[20] P.R. Murray, E.J. Baron, F.C. Pfaller, R.H. Tenover, Yolke manual of clinical microbiology, sixth ed., Am. Soc. Microbiol., Washington, DC, 1995.
[21] S. Alyar, U.Ö. Özmen, N. Karacan, O.Ş. Şentürk, K.A. Udachin, J. Mol. Struct. 889 (2008) 144.
[22] G. Ferguson, C. Glidewell, J. Chem. Soc. Perkin Trans. 2 (1988) 2129.
[23] E.M. Zerbe, O. Moers, P. G Jones, A. Blaschette, Z. Naturforsch. 60 (2005) 125.
[24] M.J. Frisch, G.W. Trucks, H.B.Schlegel, G.E. Scuseria, M.A.Robb, J.R. Cheeseman, J.A. Montgomery Jr., T.Vreven, K.N. Kudin, J.C. Burant, J.M. Millam, S.S. Iyengar, J. Tomasi, V. Barone, B. Mennucci, M. Cossi, G. Scalmani, N. Rega, G.A. Petersson, H. Nakatsuji, M. Hada, M. Ehara, K. Toyota, R. Fukuda, J. Hasegawa, M. Ishida, T. Nakajima, Y. Honda, O. Kitao, H. Nakai, M. Klene, X. Li, J.E. Knox, H.P. Hratchian, J.B. Cross, C. Adamo, J. Jaramillo, R. Gomperts, R.E. Stratmann, O. Yazyev, A.J. Austin, R. Cammi, C. Pomelli, J.W. Ochterski, P.Y. Ayala, K. Morokuma, G.A. Voth, P. Salvador, J.J. Dannenberg, V.G. Zakrzewski, S. Dapprich, A.D. Daniels, M.C. Strain, O. Farkas, D.K. Malick, A.D. Rabuck, K. Raghavachari, J.B. Foresman, J.V. Ortiz, Q. Cui, A.G. Baboul, S. Clifford, J. Cioslowski, B.B. Stefanov, G. Liu, A. Liashenko, P. Piskorz, I. Komaromi, R.L. Martin, D.J. Fox, T. Keith, M.A. Al-Laham, C.Y. Peng, A. Nanayakkara, M. Challacombe, P.M.W. Gill, B. Johnson, W. Chen, M.W. Wong, C. Gonzalez, and J.A. Pople, Gaussian 03, Revision B.04,Gaussian, Inc., Pittsburgh, PA, 2003.
[25] HyperChem 7.5 program, Hypercube Inc., Toronto, Canada, 2002.
[26] A.S. Baranski, W.R. Fawcett, C.M. Gilbert, Am. Chem. Soc. 57 (1985) 166.
[27] C. Santelices, M.D. Hawley, J. Electroanal. Chem. Interfacial Electrochem. 84 (1977) 387.